Design of an ILS localizer for the new Montijo Airport

Sara A. Rodrigues, *Instituto Superior Técnico, Portugal*

***Abstract*—The aim of this paper is to study the implementation of a localizer from the Instrument Landing System (ILS) in the new Montijo Airport. For this purpose, it is necessary to understand all the system and to know how a localizer works. Since the localizer is formed by an array of Log-Periodic-Dipole (LPD) antennas it is important to study the characteristic parameters of antennas and the features of the arrays and LPD antennas. After acquiring all the knowledge regarding these themes, the configuration of LPD antenna is determined, as well as the array that best suits the particularities of the new airport, always complying the requirements imposed by International Civil Aviation Organization (ICAO). Lastly, the electric field at the receiver location is analyzed, considering the reflections on the ground and its roughness and diffractions caused by obstacles. All of these radio propagation phenomena are studied taking into account that the final electric field needs to be larger than the receiver's sensitivity.**

***Index Terms* - Antenna arrays, Instrument Landing System, Localizer, Log-Periodic-Dipole antennas.**

I. Introduction

Bird watching has always caused curiosity and admiration in mankind. This fascination led Man to study the basic principles of flying and to do experiments in this area. After the Wright's brothers had flown with a device heavier than air, many advances and discoveries were made in aviation. Nowadays aviation has advanced radio navigation aids such as the Instrument Landing System (ILS) of which the localizer system is part. Since the ILS is very complex, this paper begins with the analysis of the system. After understanding the system this work focuses on the detailed study of localizer. For this purpose, it was necessary to get knowledge of the characteristic parameters of the antennas, the radio propagation phenomena, the particularities of arrays and the operating mode of Log-Periodic-Dipole (LPD) antennas. After acquiring all the fundamental concepts, the array and LPD configurations were chosen so that they had the characteristics that best fit the new airport, always bearing in mind that the emitted field must be greater than the receiver sensitivity.

II. Fundamental Concepts

A. Instrument Landing System

The ILS requires two main systems, a localizer (LOC) that provides azimuth and a glide slope (GS) that defines the vertical descent profile [1]. These systems radiate continuous radio frequency waves horizontally polarized [2]. The LOC has 40 channels in the 108-112 MHz (VHF) band and the assigned frequencies correspond to odd decimal numbers and the same summed up to 0.05 MHz (e.g.: 108.1 108.15 108.3 108.35… 111.95 MHz). GS also has 40 channels in the 329.15-335 MHz (UHF) band, and their frequencies are spaced by 0.15 MHz (e.g.:329.15 329.3 329.45… 335 MHz) [1].

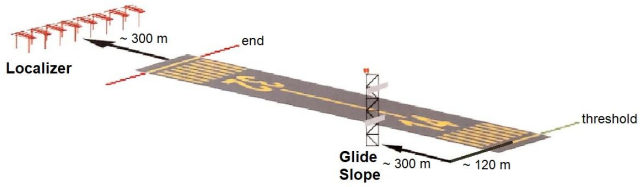

Fig. 1 - LOC and GS locations relative to runway.

LOCs are linear arrays composed of at least 6 log-periodic antennas. These arrays can have 12 to 40 meters long, 3 meters high and are usually placed about 300 meters after the end of the runway with their axis perpendicular to the centerline of the runway (Fig. 1) [2]. The radiation diagram emitted by the localizer results from the combination of two amplitude modulated signals one with 90 Hz and other with 150 Hz. It is through the Difference in Depth of Modulation (DDM) analysis that the airborne equipment can measure which is the deviation of the aircraft from the centerline of the runway. If the aircraft is to the right the 150 Hz tone will predominate indicating that the aircraft must travel to the left to reach the runway axis. If it is on the left side the 90 Hz tone will prevail meaning that the displacement must be to the right (Fig. 2). In the plane that contains the axis runway (course line) there is a balance between the two modulations resulting in a zero DDM.

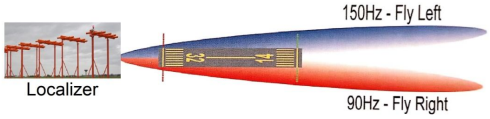

Fig. 2 - 90Hz and 150Hz signals relatively to the runway in the horizontal plane.

The LOC signals are only reliable up to a distance of 25 nautical miles (NM) and an altitude of at least 600 m from the horizontal plane containing the threshold. In Fig. 3 we can see that at a distance of 25 NM (46.3 km) the coverage extends

S. A. Rodrigues, from Instituto Superior Técnico, Lisboa, Portugal (saraarodrigues@tecnico.ulisboa.pt)

10º to each side of the runway centerline and from 10º to 35° when the distance is 17 NM (31.5 km). In all parts of the coverage the field strength shall not be less than 40μV/m [3].

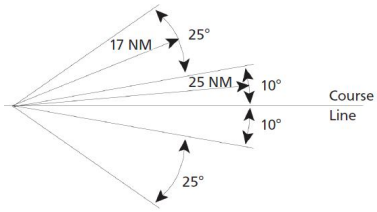

Fig. 3 – Localizer coverage [4].

The GS is constituted by two or three antennas arranged on a vertical mast that use the ground plane to form a mirror image of the mast. This effect results in a system with twice of the antennas seen above the surface [5].

The GS mast can be up to 15 meters high and is usually placed on one side of the runway 120 meters from the center line and about 300 meters after the threshold [4]. GS system also use DDM to identify the position of the aircraft, in this case for the vertical plane. When 90 Hz tone predominates the aircraft receives indications that it is above the glide path and therefore must move downwards. Whenever 150 Hz tone prevails, the aircraft is positioned below the glide path and is advised to shift upwards (Fig. 4). The glide path is the line where the modulations have the same intensity, i.e., the DDM is equal to zero. This line is 3° from the horizontal but according to ICAO requirements it may be between 2° and 4° [1]. The 3° angle leads to a glide path with an altitude of approximately 15 meters at the threshold.

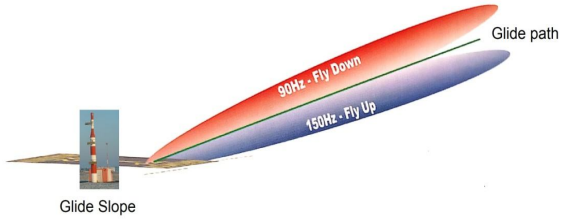

Fig. 4 - 90Hz and 150Hz signals relatively to the runway in the vertical plane.

During the approach process pilots start by following the ILS guidelines until they reach the decision height (DH). When this height is reached the approach to the runway can only be performed if the runway visual range (RVR) is above the stipulated minimum otherwise a deviation must be performed and the approach procedure fails [4]. Aircrafts may operate in one of the following categories:

• CAT I - defines that the DH cannot be less than 60 m and with either a visibility not less than 800 m or a RVR not less than 550 m;

• CAT II - allows a minimum DH of 30 m and a minimum RVR of 300 m;

• CAT IIIA - without DH limit and a minimum RVR of 175 m;

• CAT IIIB - without DH limit and a minimum RVR of 50 m;

• CAT IIIC - fully automatic landing without DH or RVR limitations [6].

In order to operate in categories II and III the aircraft must have appropriate flight characteristics, the airport needs to be properly equipped and the crew shall be qualified according to the categories to be used [4]. Higher categories require more accurate equipment since the information provided has to be reliable for smaller heights. The categories are chosen according to factors such as traffic density, weather conditions and obstacles in the vicinity of the runway [7].

B. Characteristic parameters of antennas

1) Radiation diagram

The radiation diagram of an antenna is a "mathematical function or graphical representation of the radiation properties of the antenna as a function of spatial coordinates" [8]. These diagrams are composed for several lobes where the main lobe corresponds to the region with the maximum radiation and the secondary lobes the remaining radiation regions. In the radiation diagram it is possible to determine the half power beamwidth and the beamwidth between nulls. The first one represents the angle between the two directions where the radiation intensity is half of the maximum value and the second one corresponds to the angle between directions of nulls. Another important parameter to determine is the side lobe level (SLL) that results from the comparison between the maximum intensity of the main lobe with the maximum intensity of the largest secondary lobe [9]. For most the applications the SLL should be less than -20 dB [8].

2) Directivity

Directivity corresponds to the ratio between the radiation intensity in a given direction (U) and the average radiation intensity in all directions (U_0). This ratio corresponds to the following expression:

$$D = \frac{U}{U_0} = \frac{4\pi U}{P_{rad}} \quad (1)$$

3) Efficiency

Due to losses in the conductors not all the power delivered to the antenna (P_e) is radiated (P_{rad}). According to [9], the efficiency corresponds to the relation between these two powers:

$$\eta = \frac{P_{rad}}{P_e} \quad (2)$$

When mismatch losses are taking into account, i.e., input (Z_{in}) and transmission line (Z_0) impedances do not match due to transmission line reflections, we have the total efficiency:

$$e = \eta(1 - |s_{11}|^2) \quad (3)$$

Where s_{11} represents the reflection coefficient and is given by:

$$s_{11} = \frac{Z_{in} - Z_0}{Z_{in} + Z_0} \quad (4)$$

4) Gain

The gain is a parameter that takes into account the antenna performance and its directional properties [8]. Since directional properties are measured through the directivity, the gain is determined as follows:

$$G = \eta D \quad (5)$$

5) Voltage Standing Wave Ratio

Voltage Standing Wave Ratio (VSWR) is the ratio between the maximum (V_{max}) and minimum (V_{min}) voltages on the transmission line:

$$VSWR = \frac{V_{max}}{V_{min}} \tag{6}$$

If there were ideal systems the voltage would be constant ($V_{max} = V_{min}$) and consequently the VSWR would be equal to 1. However this never happens due to transmission line reflections that cause changes in voltage. Since voltage depends on the transmission line reflections VSWR can also be written as a function of the reflection coefficient [9]:

$$VSWR = \frac{1 + s_{11}}{1 - s_{11}} \tag{7}$$

Observing (4) and (7) it is visible that greater differences between input and transmission line impedances result in higher values of reflection coefficients and VSWR.

For most systems it is acceptable to have reflections up to 10%, i.e., the VSWR must be less than 2 and the reflected power less than -10 dB [9].

6) Polarization

When an electric current travels through an antenna two fields are generated: the electric field in the same plane of the current flow and the magnetic field in the perpendicular plane of the flow.

Since the polarization is defined by the plane of the electric field, vertical antennas have vertical polarization since the current travels vertically. Following the same reasoning horizontal antennas produce horizontal polarizations.

To receive the maximum signal strength the receiving antenna must be in the same plane as wave polarization [4].

7) Bandwidth

The antenna bandwidth corresponds to the frequency range where its characteristics meet the specifications of use [10]. This is usually defined as a percentage:

$$LB_{\%} = \frac{f_{max} - f_{min}}{f_0} \times 100\ [\%] \tag{8}$$

Where f_{max} and f_{min} correspond respectively to the maximum and minimum frequencies and f_0 to the center frequency. The center frequency is obtained from:

$$f_0 = \frac{f_{max} + f_{min}}{2}\ [\text{Hz}] \tag{9}$$

C. Linear antenna array

A linear antenna array is a set of similar antennas arranged along a straight line that have specific phase and amplitude to achieve certain radiation characteristics [11]. These antennas are designed to have high gains that are obtained by combining the fields of the different elements in a constructive way in the desired direction and destructively in the other directions.

In mathematical terms, the total field of an array is calculated by multiplying the field of a single element by the array factor. Each array has its own array factor that varies according the number of constituent elements, their spatial arrangement, their relative magnitudes and phases and spacing between them.

The arrays can be designed by uniforms or non-uniforms. In the uniform arrays all elements have the same amplitude, are equidistant (d) and have progressive phases [10].

Let's now analyze an uniform array with two infinitesimal horizontal dipoles distanced by d and fed by currents with equal amplitude and phase difference β. The Fig. 5 shows that element 2 has a delay of $d\cos\theta$ which leads to a phase difference of $kd\cos\theta$. Adding the initial phase difference between the elements (β) we stay with a total phase difference of:

$$\Delta\psi = \frac{2\pi}{\lambda} d\cos\theta + \beta\ [\text{rad}] \tag{10}$$

Having the phase difference between the elements and knowing that they have equal amplitudes we get the following electric fields:

$$E_1 = E_0 \cos\theta_1\, e^{j\frac{\Delta\psi}{2}} \tag{11}$$

$$E_2 = E_0 \cos\theta_2\, e^{-j\frac{\Delta\psi}{2}} \tag{12}$$

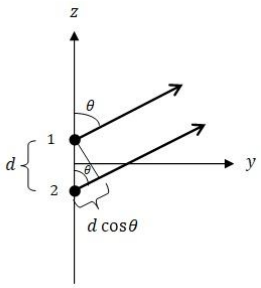

Fig. 5 - Distant field geometry of an uniform array with two infinitesimal horizontal dipoles positioned along the z axis.

The total electric field corresponds to the sum of the fields produced by the different elements. So, for far-field observations ($\theta_1 = \theta_2 = \theta$) it is:

$$E_t = E_1 + E_2 = 2E_0 \cos\theta \cos\left(\frac{\Delta\psi}{2}\right) \tag{13}$$

Through the analysis of (13) it is possible to corroborate what is mentioned in [11], that the total field of an array composed by identical elements results from the multiplication of the element factor by the array factor (principle of pattern multiplication). For this case the element factor corresponds to the field radiated by one of the infinitesimal horizontal dipoles ($E_0\cos\theta$) and the array factor is given by:

$$FA = 2\cos\left(\frac{\frac{2\pi}{\lambda} d\cos\theta + \beta}{2}\right) \tag{14}$$

D. Log-Periodic-Dipole antennas

The LOC system uses LPD antennas in their constitution because they have customizable bandwidth and directive characteristics [12].

A LPD is a linear array of half-wave dipoles that are connected in ascending order of length. The shortest elements are in the front of the antenna, where the power is provided, and the longest elements at the end [13].

LPD antennas operate at VHF and UHF frequencies covering from 30 MHz to 3 GHz. They do not operate at higher frequencies because it would require the production of such small dipoles that it is not feasible [14].

On these antennas, the lengths (l_n), the spacings (R_n), the diameters (d_n) and the spacings at the center of the dipoles (s_n) are related through the geometric ratio (τ):

$$\frac{1}{\tau} = \frac{l_{n+1}}{l_n} = \frac{R_{n+1}}{R_n} = \frac{d_{n+1}}{d_n} = \frac{s_{n+1}}{s_n} \quad (15)$$

LPDs are also characterized by the spacing factor (σ) obtained from:

$$\sigma = \frac{R_{n+1} - R_n}{2l_{n+1}} \quad (16)$$

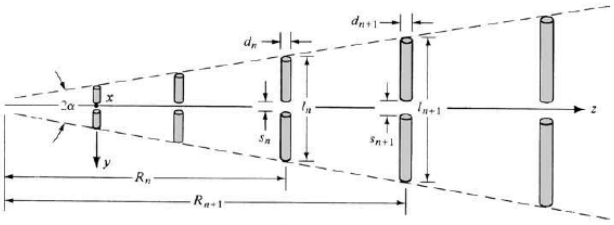

Fig. 6 - Log-periodic-dipole structure [8].

Fig. 6 shows that the two lines that connect the tips of all dipoles form a vertex angle of 2α, where α corresponds to:

$$\alpha = \tan^{-1}\left[\frac{1-\tau}{4\sigma}\right] [°] \quad (17)$$

LPD antenna designs typically use half vertex angles of $10° \leq \alpha \leq 45°$ and geometric ratios of $0.95 \geq \tau \geq 0.7$ [8].

LPDs are powered by a source that is connected to a transmission line. This transmission line cross-connects adjacent dipoles to feed them with opposite phases [11]. So, the smallest and closest elements will radiate little energy as their phases cancel each other out and the largest and most distant dipoles are responsible for the radiation of much of the energy. This phase inversion between adjacent elements causes the energy to be radiated towards the shorter dipoles [8].

E. Radio propagation

1) Free space propagation

Wave propagation in free space occurs when transmission is carried out in the absence of obstacles and through a uniform medium. Under these conditions for a transmitter with gain G_e we have a received power of [15]:

$$P_r = \frac{P_e G_e G_r \lambda^2}{(4\pi d)^2} \text{ [W]} \quad (18)$$

Where P_e corresponds to the power delivered to the transmitting antenna, G_r to the gain of the receiving antenna and d to the distance between the transmitting and receiving antennas. For this transmitter the root mean square (RMS) value of the electric field is [16]:

$$E = \frac{\sqrt{30 P_e G_e}}{d} \text{ [V/m]} \quad (19)$$

2) Ground reflections

Previously it was approached the propagation in free space where only the presence of direct rays was considered. However, due to the existence of the earth it is necessary to take into account the reflected rays as they strongly alter the received signal. Since the earth is approximately spherical, a mathematical model is used to determine the range of communications. This model transforms the spherical earth problem into a flat earth problem by using equivalent heights (h') [17]. Since this model considers flat ground the reflection occurs only at one point (specular point) with no energy dissipated in other directions. This terrain characteristic results in a reflection angle equal to the incidence angle and a propagation of the reflected wave in the same plane as the incident wave direction [18].

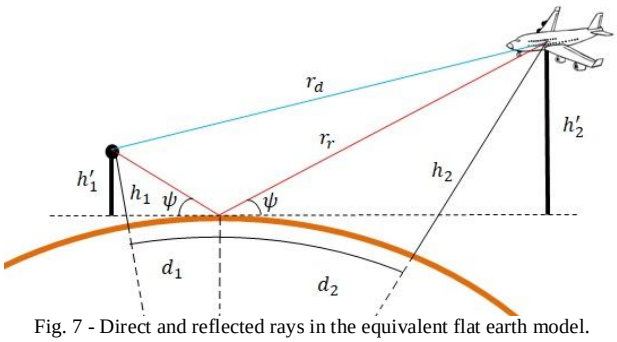

Fig. 7 - Direct and reflected rays in the equivalent flat earth model.

As we can see in Fig. 7 the incidence angle is given by:

$$\psi = tan^{-1}\left(\frac{h_1' + h_2'}{d}\right) [°] \quad (20)$$

This angle depends on the equivalent heights of the transmitting (h_1') and receiving (h_2') antennas which come from:

$$h_1' = h_1 - \frac{d_1^2}{2a_e} \text{ [m]} \quad (21)$$

$$h_2' = h_2 - \frac{d_2^2}{2a_e} \text{ [m]} \quad (22)$$

Where a_e corresponds to the equivalent radius of the earth which depends on the radius of the earth (6370 km) and the constant for a standard atmosphere (K=4/3).

$$a_e = aK \text{ [m]} \quad (23)$$

According to [17] the distance between the transmitting antenna and the specular point (d_1) is given by:

$$d_1^3 - \frac{3}{2}d d_1^2 + \left[\frac{1}{2}d^2 - a_e(h_1 + h_2)\right] d_1 + h_1 d a_e = 0 \quad (24)$$

Therefore the distance from the specular point to the receiving antenna is equal to:

$$d_2 = d - d_1 \text{ [m]} \quad (25)$$

The reflected fields are given by Fresnel coefficients that have the following expression for horizontal polarization [18]:

$$\Gamma_H = \frac{\sin(\psi) - \sqrt{n^2 - \cos(\psi)^2}}{\sin(\psi) + \sqrt{n^2 - \cos(\psi)^2}} \quad (26)$$

The variable n corresponds to the ground to air reflection index and is given by:

$$n = \left(\frac{\varepsilon_s'}{\varepsilon_0}\right)^{\frac{1}{2}} \quad (27)$$

In (27) ε_0 express the permittivity of air taken to be equal to the vacuum, i.e., 8.854×10^{-12} F/m. The symbol ε_s' represents the complex dielectric permittivity of the ground that corresponds to:

$$\varepsilon_s' = \varepsilon_s - j\frac{\sigma_s}{\omega} \text{ with } \varepsilon_s = \varepsilon_r \varepsilon_0 \; e \; \omega = 2\pi f \quad (28)$$

Where ε_r is the relative permittivity and σ_s the ground conductivity [17].

In order to determine the resulting phase difference between the direct and reflected fields ($\Delta\phi$) it is necessary to calculate the path difference (Δr) between the direct (r_d) and reflected (r_r) rays [15]:

$$r_d = \sqrt{d^2 + (h'_2 - h'_1)^2} \text{ [m]} \quad (29)$$

$$r_r = \sqrt{d^2 + (h'_2 + h'_1)^2} \text{ [m]} \quad (30)$$

$$\Delta r = r_r - r_d \text{ [m]} \quad (31)$$

$$\Delta\phi = \arg(\Gamma) - 2\pi\frac{\Delta r}{\lambda} \text{ [rad]} \quad (32)$$

The total field at the receiver location results from overlapping the direct field (E_d) with the reflected field (E_r) [17]:

$$E = E_d + E_r = E_d\left(1 + \frac{\sqrt{G_{rr}}|\Gamma_H|D_{iv}e^{j\Delta\phi}}{\sqrt{G_{rd}}}\right) \text{ [V/m]} \quad (33)$$

Where G_{rd} and G_{rr} correspond respectively to direct and reflected ray gains.

Since the Fresnel coefficients consider reflections on flat surfaces and in reality, they occur on a spherical surface, the expression (33) takes into account the divergence factor (D_{iv}) which represents the extent to which the reflection on the spherical surface disperses more energy than on a flat surface. According to [15] this factor is given by:

$$D_{iv} = \frac{1}{\left(1 + \frac{2d_1d_2}{a_e d\sin\psi}\right)^{1/2}} \quad (34)$$

a) Rough ground

When the terrain where the reflection takes place is not flat there is energy dispersion in several directions. This scatter can cause changes in the field so it is preponderant to analyze how the field is affected by it. The notions of flat and rough depend on wavelength, i.e., the same ground can be considered rough for short wavelengths and flat for large wavelengths [17].

According to Rayleigh's criterion a terrain is considered flat when the phase difference between two points of it is much smaller than π:

$$g = kd = \frac{4\pi h_p}{\lambda}\sin\psi \ll \pi \text{ [rad]} \quad (35)$$

Where h_p represent the difference of height between the two points of the ground.

Hereupon, for $h_1, h_2 \ll d$ the field is obtained by [19]:

$$E = E_d\left(1 + |\Gamma|D_{iv}e^{j\Delta\phi}e^{-g^2/2}\right) \text{ [V/m]} \quad (36)$$

3) Diffraction caused by obstacles

For the study of diffraction caused by obstacles the knife-edge model is used.

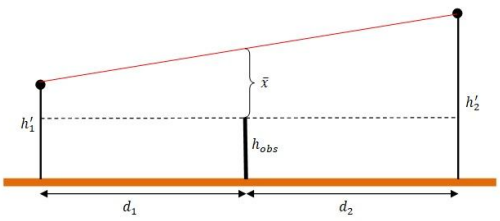

Fig. 8 - Knife-edge model.

This model argues that to avoid interference caused by an object the direct ray must be in line of sight and the Fresnel ellipsoid needs to be unimpeded. Thus, the clearance ($\bar{x}$) between the direct ray and the obstacle must be greater than the radius of the 1st Fresnel ellipsoid, i.e. [16]:

$$\bar{x} > R = \sqrt{\frac{\lambda d_1 d_2}{d}} \text{ [m]} \quad (37)$$

Where the clearance corresponds to [19]:

$$\bar{x} = \frac{(h'_1 - h_{obs})d_2 + (h'_2 - h_{obs})d_1}{d} \text{ [m]} \quad (38)$$

When the condition (37) is not met the signal is attenuated. This attenuation varies with the equivalent height (Fig. 9) which is determined through:

$$h_e = \sqrt{\frac{2d}{\lambda d_1 d_2}}\bar{x} \quad (39)$$

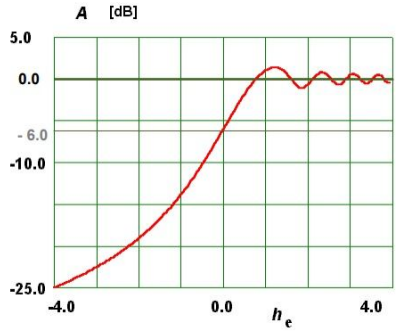

Fig. 9 - Attenuation introduced by a knife-edge obstacle as a function of equivalent height [19].

III. Localizer System

A. Localizer generated sector

It is through the difference between the 90 and 150 Hz (DDM) modulations that it is known which direction the aircraft must take. The pilot has access to this information on the Course Deviation Indicator (CDI) which shows the deviation of the aircraft relatively to the centerline of the runway. The sector that contains the maximum deviations that CDI can display in both directions is called Course Sector (CS). According [5] this sector is given by:

$$CS = 2\tan^{-1}\left(\frac{105}{d}\right) \text{ [°]} \quad (40)$$

Observing (40) we note that it is the distance between the localizer and the threshold (d) that defines the size of the CS. According to ICAO Course Sectors can range from 3º to 6º and on your edges the DDM must be 0.155.

B. Modulation

The LOC signal is generated from an oscillator that emits a carrier of approximately 110 MHz. This signal is further divided into two equal parts to power two modulators where the carrier is modulated at 150 Hz and 90 Hz with 40% deep. These modulated signals are then combined in phase and in out-of-phase resulting in two signals: Carrier and Side Bands (CSB) and Side Bands Only (SBO).

We will consider the example of Fig. 10 where the carrier has an amplitude of 100 and each tone an amplitude of 40 (40% of the carrier level).

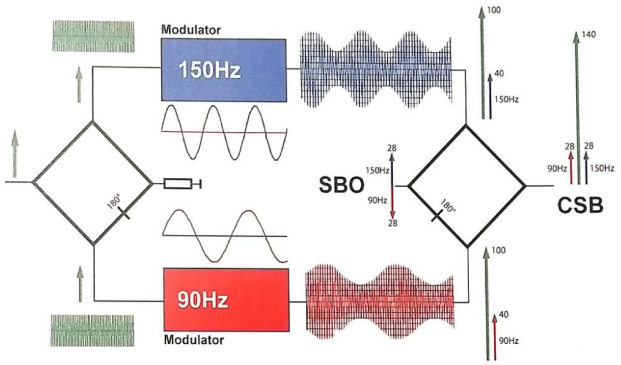

Fig. 10 - Formation of CSB and SBO signals [5].

In CSB the modulated signals combine in phase so the carriers add up resulting in a signal with amplitude of approximately 140 (twice of the power of 100) [5]. When we add the two bands of 90 Hz and 150 Hz signals, the CSB tones stay with half of the initial signal strength, i.e., with amplitude 28 (half of the power of 40).

Using the modulation expression in (41) where T corresponds to the amplitude of each tone and P to the carrier amplitude it is possible to verify that in CSB signal the tones are modulated with 20% deep ($m_{90/150} = 28/140 = 0.2$) which corresponds to half of the initial modulation.

$$m_t = \frac{T}{P} \tag{41}$$

For SBO as the signals are in out-of-phase the carriers cancel each other out and the tones divide into their new bands, also with amplitudes of 28 but with opposite phases (Fig. 10). Thus the 150 Hz CSB and SBO tones are in phase while the 90 Hz tones are in out-of-phase.

Since the CSB signal has the same modulation for both tones (20%) it will have a modulation difference of zero. This zero DDM will indicate that the aircraft is at the centerline of the runway. Thus the CSB signal alone would not be very useful once we intent to have different indications to the various positions of the aircraft. That is why the SBO is used simultaneously, a signal whose the DDM values are opposite for each side of the runway, allowing to know which side of it the aircraft is in. Besides that, SBO signal decrease his intensity with the proximity to the center showing how far the aircraft is from the centerline [5].

C. DDM

As seen earlier, in the CSB signal the modulation difference between the 90 and 150 Hz tones is 0% however when this signal mixes with the SBO this difference will change. Since the SBO tones are in out-of-phase the combination will make one of the CSB tones increase and the other decrease. Thus, the final DDM will correspond to the difference between the resulting modulations from the junction of CSB and SBO signals [3]:

$$DDM = \frac{m_{150} - m_{90}}{100} \tag{42}$$

Depending on which side the aircraft is in relation to the center of the runway the DDM may have positive or negative values (Fig. 11). On the right side as the 150 Hz tones of the CSB and SBO signals are in phase this modulation will predominate resulting in a positive DDM. When the aircraft crosses the center line and transits to the left side of the runway, the phase of the SBO changes 180º. Therefore the 90 Hz tones of both signals will be in phase. So the 90 Hz modulation will prevail and the DDM values will be negative.

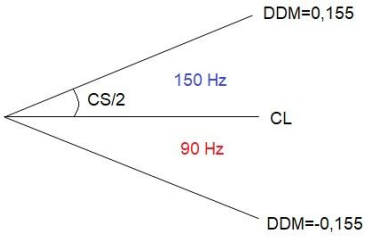

Fig. 11 - DDM distribution in localizer.

DDM can also be calculated using the CSB and SBO phasors directly. In this case the expression is [20]:

$$DDM = \frac{2 \times SBO}{CSB} \cos\varphi \tag{43}$$

Where SBO is amplitude of one of the SBO tones, CSB is the carrier amplitude in the CSB signal and φ the phase difference between the 150 Hz tones of the two signals.

D. Array Characteristics

The localizer corresponds to a linear array of LPD antennas. Although the number of elements may be odd, LOCs are generally made up of an even number of LPD antennas that are grouped in pairs. The antennas are paired together forming uniform 2-element linear arrays however the localizer is considered a non-uniform array because each pair has its own amplitude and distance between antennas. Since the reference point of this system corresponds to the center of the array, the antennas are grouped two by two from the center to the periphery.

In this non-uniform system the total array factor will correspond to the sum of each antenna pair array factors [20]:

$$FA_{total} = \left| \sum_{p=1}^{P} 2A_p \cos\left(\frac{kd_p \cos\theta + \beta}{2}\right) \right| \tag{44}$$

Where P is the number of antenna pairs and A_p the feed amplitude of each pair.

Regarding the radiation diagram of the array we saw in chapter II that it results from the multiplication of the array factor by the field emitted by one of the elements. Knowing that localizer elements correspond to LPD antennas and that they are fed with the CSB and SBO signals, a two-component radiation diagram is obtained:

$$E_{CSB}(\theta) = FA_{CSB}(\theta) \times E_{LPD}(\theta)\ [\mathrm{V/m}] \tag{45}$$

$$E_{SBO}(\theta) = FA_{SBO}(\theta) \times E_{LPD}(\theta)\ [\mathrm{V/m}] \tag{46}$$

Regarding the feeding amplitudes, they are chosen to generate the best radiation diagram. This diagram should not only comply ICAO requirements but also be optimized for the LOC implementation site. Given the extensive studies that have already been performed, standard feed values are available for some of the most commonly used LOC designs. These values are optimized in relation to the number of elements used in each system and the corresponding value of the CS.

E. LPD antenna analysis

In this subchapter we used Antenna Magus and CST Studio Suite software to analyze different LPD antenna configurations.

We started by exporting an LPD antenna in Antenna Magus already adjusted to the operating band of the localizer, i.e., from 108 to 112 MHz. After that it was necessary to define some parameters such as center frequency, percentage bandwidth, gain and input resistance. For the center frequency we assign the value of 110 MHz. With this value we determined the percentage bandwidth using the expression (8). Although we had obtained a bandwidth of approximately 3.64% we chose the value 20% because usually the projected bandwidths are bigger than the bands really needed.

To evaluate the effect of gain several designs were created with different values for this parameter. Regarding the input resistance we used a constant value of 200 Ω.

After analyzing all the models we concluded that higher gains imply higher number of elements and result in lowest values of the VSWR in the antenna operating band (Fig. 12).

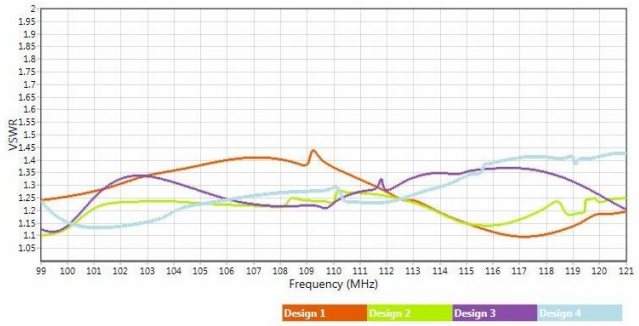

Fig. 12 - VSWR for designs 1, 2, 3 and 4 with gains 8, 10, 12 and 9.5 dB respectively (image created by Antenna Magus software).

Since the VSWR values of the 2, 3 and 4 designs are very close, we chose the one with 9.5 dB because it uses fewer elements.

Then, to study the effect of the input resistance we created new designs with a constant gain of 9.5 dB and different values of resistance. In this case we concluded that higher input resistance values imply more elements. Regarding the VSWR, very close values were obtained so we exported the 3 models (with 100, 200 and 300 Ω) to CST software in order to perform a more rigorous analysis. Looking at the reflected power values of the 3 models we conclude that by increasing the input resistance, the reflected power values get higher and consequently the VSWR also increases. Since we want the lowest VSWR (close to 1) and the LPD with the fewest elements, we chose the model with 100 Ω.

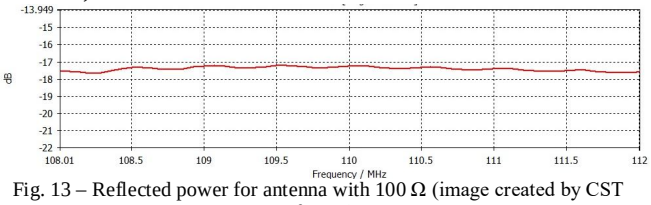

Fig. 13 – Reflected power for antenna with 100 Ω (image created by CST software).

As we can see in Fig. 13 this antenna has excellent values for reflected power, which are always below -17 dB. This means that the reflections are less than 2% what is quite good since up to 10% reflection powers are acceptable.

In Tab. 1 We can see the various parameters of the chosen antenna.

Tab. 1 - Characteristics of an LPD with f_0 = 110 MHz, $LB_{\%}$ = 20%, G = 9.5 dB and R_{in} = 100 Ω.

Elements	s[mm]	τ	σ	l_N[m]	$d_N/2$ [mm]
9	10.44	0.917	0.193	1.560	4.407

IV. Project Definition

A. Montijo Airport

The current Montijo Airport is made up of two runways, 1/19 and 8/26. For the new airport will be used the 1/19 runway because its orientation is practically parallel to runway 3/21 of Humberto Delgado Airport, allowing the take off or land of two aircraft at the same time [21]. The main runway (8/26) will continue for military flights.

We used the Google Earth Pro software for measuring the runway and we obtained a length of 2187 m and a width of 44 m. According to [22], the current runway length is not sufficient for large aircraft to take off. So an increase of the runway to 2400 m is predicted. Since it starts and ends very close to the estuary, this increase will only be possible through the creation of a landfill. According to Montijo's mayor, it is possible to create a 500 m landfill in direction to Barreiro without much environmental impact. Hereupon, with the creation of the landfill, it is possible to have a 2400 m runway with localizers positioned at 263 m for each side of it.

B. Definition of array characteristics

A new prefabricated structure similar to Terminal 2 of Humberto Delgado Airport will be installed at the new Montijo Airport [21]. Since this structure is relatively small compared to the whole Lisbon Airport, we decided to use a LOC with 12 LPD antennas, which corresponds to half of the elements used in Humberto Delgado Airport localizer.

To obtain the feeding amplitudes and antenna spacing of the CSB and SBO signals we resort to [20] where we can find the optimal values for 12-element localizers with CS of 4º.

In order to verify if this configuration fits the new Montijo Airport we calculated its CS using expression (40). Since the runway has 2400 m and the LOC is located 263 m from the end of the runway we have a CS of approximately 4.5º ($2\tan^{-1}(105/2663) \cong 4.5°$). Given the difference in the course sectors we had to adjust the SBO signal amplitudes. To do that, we first determine the pattern of the CSB array factor for various angles inserted in CS/2. For this purpose we used the data related to the CSB present in Tab. 2 and the expression (44). With this we obtained the Fig. 14 where we can verify that in the limit of the CS (92.25º) the CSB is 375.8%.

Tab. 2 - Amplitude, spacing and phase values of the CSB signal, optimized for a 12 antenna LOC with a 4º CS.

Pairs	1º	2º	3º	4º	5º	6º
Spacings [m]	1.90	9.54	15.82	21.80	27.80	33.80
CSB amplitudes [%]	100.0	54.90	33.50	19.00	8.10	2.40
CSB phases [º]	0	0	0	0	0	0

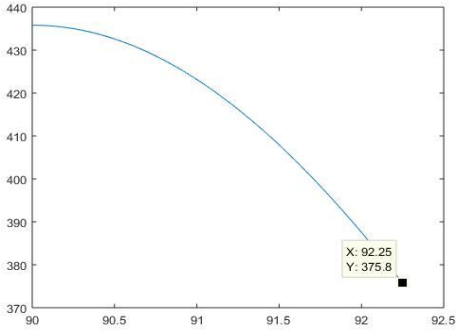

Fig. 14 – Pattern of CSB array factor [%] for angles θ insert in CS/2.

So, since we know that in this limit the DDM is 0.155 and the phase difference between the 150 Hz tones of CSB and SBO signals corresponds to zero, it is possible to determine the value of the SBO through expression (43).

$$SBO = \frac{DDM \times CSB}{2} = \frac{0.155 \times 375.8}{2} \cong 29.12\%$$

Knowing the value that SBO must have at θ = 92.25° we adjusted its feeding amplitudes until we obtain an array factor of 29.12% for this angle. This value was obtained using the feeding amplitudes of Tab. 3 in (44).

Tab. 3 – Amplitude and phase values of the SBO signal, optimized for a 12 antenna LOC with a 4.5º CS.

Pairs	1º	2º	3º	4º	5º	6º
SBO amplitudes [%]	7.10	5.00	6.72	4.88	2.61	0.90
SBO phases [º]	180	180	180	180	180	180

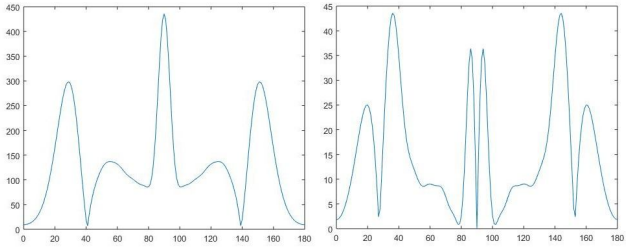

Fig. 15 - Array factors patterns [%] of CSB and SBO signals as a function of θ.

After adjusting the SBO amplitudes according to the characteristics of the Montijo Airport runway, we determined the array factor patterns of the CSB and SBO signals for all θ values. These patterns are shown in Fig. 15. Next we resorted to the CST in order to obtain the electric field emitted by the LPD chosen in chapter III (Fig.16).

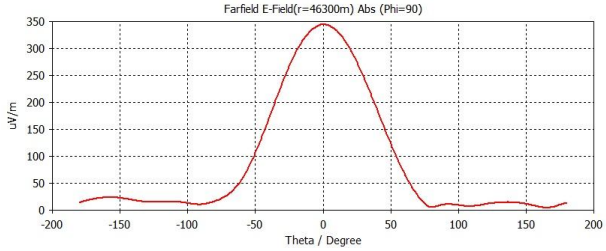

Fig. 16 - Electric field [μV/m] for a LPD with a 9.5 dB gain, 100 Ω input resistance and 1 W excitation.

As seen before, the LOC radiation diagram has two components the $E_{CSB}(\theta)$ and $E_{SBO}(\theta)$. For their determination we used (45) and (46), with the array factors of CSB and SBO divided by 100 to be in linear values instead of in percentage. As a result we obtained the electric field radiation diagram represented in Fig. 17.

In the aircraft these two components are received in the form of DDM. So we represented the DDM, as a function of θ, using the values of the two components in expression (43).

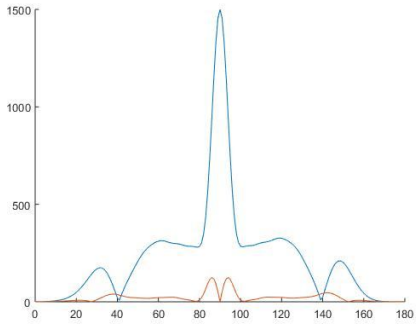

Fig. 17 - $E_{CSB}(\theta)$ and $E_{SBO}(\theta)$ components of the electric field emitted by the localizer [μV/m].

In Fig. 18 we can see that on the left side of the runway DDM values are negative and on the right side are positive, i.e., at the center line of the runway (θ = 90°) the 150 Hz tone's phase of the SBO signal reverses 180°.

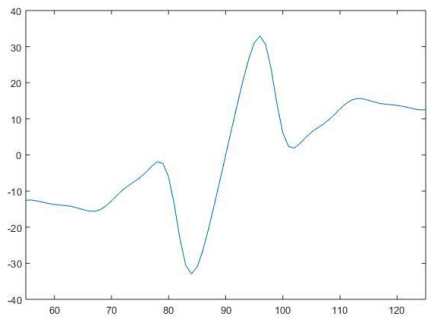

Fig. 18 - DDM [%] as a function of θ.

C. Electric Field at receiver's location

In this subchapter we intend to determine the field in the receptor's location taking into account some radio propagation phenomena that cause changes in its values.
We started with the study of the electric field when ground reflections occur. Using the expressions present in the subchapter "Ground reflections" we obtained the electric field present in Fig. 19.

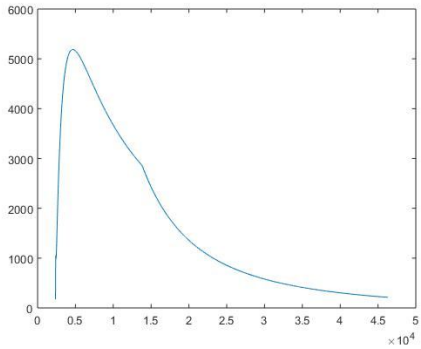

Fig. 19 - Electric field [μV/m], resulting from the overlapping of the direct and reflected fields, as a function of the distance [m].

Observing Fig. 19 we conclude that there is no coverage problems since the minimum field value ($170.8\,\mu V/m$) is higher than the receiver sensitivity ($6.232\,\mu V/m$).
Regarding the ground, we found that it is considered flat since the phase difference between two terrain points, with a height of 1 cm, is always much smaller than π (Fig.20)

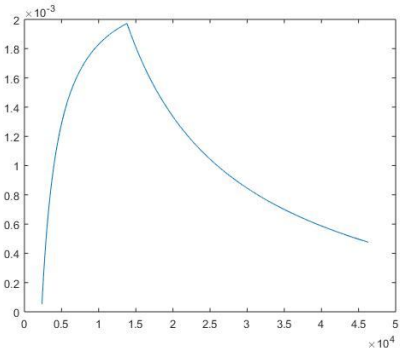

Fig. 20 - Phase difference between two terrain points [rad] as a function of distance [m].

Then we analyzed the diffraction caused by obstacles. For this purpose 4 obstacles were considered: two for the LOC installed at north of the runway and two for the LOC located at south. The first one has as obstacles the opposite LOC and one tree in Barreiro. The second one has the Vasco da Gama's bridge and the opposite LOC. Since they all have distances where the clearance is less than the radius of the 1st Fresnel ellipsoid, we determined the equivalent heights and its attenuations for the worst cases.

Tab. 4 - Obstacles characteristics.

Obstacles	**Distance to obstacle (d_1)**	**Height of obstacle (h_{obs})**
Opposite LOC	2926 m	3 m
Bridge	6470 m	20 m
Tree	6463 m	13 m

The worst case scenario occurs for a distance of 46300 m where the equivalent heights correspond to $he_{LOC} = 0.49\,m$ and $he_{bridge} = 0.56\,m$ resulting in attenuations of approximately -2.1 dB and -1.4 dB. So, since we know that the field at 46.3 km is 212.37 μV/m (Fig. 19), we get a final field of:

$$E_{south\ LOC} = 212.37 \times 10^{-2.1/20} \times 10^{-1.4/20} = 141.94\ \mu V/m$$

As this field exceeds the receiver sensitivity, the obstacles at north of runway do not cause problems in signal reception.
The obstacles of north's LOC have equivalent heights of $he_{LOC} = 0.49\,m$, which corresponds to an attenuation of -2.1 dB, and $he_{tree} = 0.64\,m$ with an attenuation of approximately -0.6 dB. Thus, the final field will be:

$$E_{north\ LOC} = 212.37 \times 10^{-2.1/20} \times 10^{-0.6/20} = 155.63\ \mu V/m$$

With this result we can conclude that the opposite LOC and the tree that are in the south of the runway do not impede the arrival of the signal to the aircraft.

V. Conclusions

The ILS enables a precision approach to the runway. The accuracy of this system depends on the type of category. The CAT IIIC is the most rigorous category since the approach to the runway is all carried out following ILS indications. In the remaining categories the aircraft only follows the ILS until the DH. At this point the approach is only performed if there is the minimum RVR required by the category that is being used. Lower categories have higher DH and consequently the accuracy of the equipment is lower. The choice of the category will depend on factors such as airport traffic density, weather conditions and the surrounding obstacles. Worse environment conditions require higher categories.

About LOC signal we note that the CSB is responsible for indicating that the aircraft is at the centerline of the runway while the SBO shows which side and how far the aircraft is from it. This information is given through the DDM which has symmetrical values for each side of the runway axis and is zero in the center. The DDM can be determined by the phasors of the CSB and SBO signals or by the difference between the modulations resulting from the junction of these signals. Positive DDM values indicate that the aircraft is on the right side of the runway and negative values on the left side. This is due to the fact that the 150 Hz tone predominates on the right side and the 90 Hz tone on the left side.

With respect to LPD we find that higher gains imply more dipoles and result in better VSWR values, i.e., closer to 1. We also conclude that by increasing the input resistance, the number of elements required is higher and VSWR has more unpleasant results, in other words, it has higher values. Given this, we chose the configuration with 9.5 dB and 100 Ω because it has a very low reflection power (less than 2%) and needs few elements for its construction.

Regarding LOC's radiation diagram, we observed that even taking into account radio propagation's phenomena such as ground reflection and diffraction caused by obstacles, the electric field was always greater than the receiver sensitivity. Thus, there are no problems in signal reception.

With the study of the localizer system we conclude that because it is constituted by an array of arrays it has a high directivity and, therefore, its antennas do not require very high power values. In this work we used 1W excitations for each LPD and there was no signal break in the receiver location.

REFERENCES

[1] Joint Aviation Authorities, "Radio Navigation – JAA ATPL Training", in Jeppesen Sanderson Inc. Neu-Isenburg, Germany, 2004.

[2] M. Kayton e W.R. Fried, "Avionics Navigation Systems", in John Wiley & Sons, Inc. (2nd ed.) Canada, 1997.

[3] International Civil Aviation Organization, "Aeronautical Telecommunications", Annex 10, Vol. 1 – *Radio Navigation Aids*. (7th ed.), Montreal, Canada, 2018.

[4] CAE Oxford Aviation Academy, "Radio Navigation – ATPL Ground Training Series", in KHL Printing Co. Pte Ltd., Singapore, 2014.

[5] R. Holm, "ILS Fundamentals", in CreateSpace. (8.1 ed.), Scotts Valley, California, USA, 2013.

[6] International Civil Aviation Organization, "Operation of Aircraft", Annex 6, Part I –.*International Commercial Air Transport - Aeroplanes* (11th ed.), Montreal, Canada, 2018.

[7] C.M. Prates, Maintenance Course – ILS, Cartil Telecomunicações e Electrónica SA, Alfragide, Portugal, 2007.

[8] C.A. Balanis, "Antenna Theory – Analysis and Design", in John Wiley & Sons, Inc. (3rd ed) Hoboken, New Jersey, USA, 2005.

[9] A. Moreira, Antenas – Theoretical Classes, Instituto Superior Técnico, Lisboa, Portugal, 2018.

[10] C. Peixeiro, Propagação e Radiação de Ondas Electromagnéticas – Theoretical Classes, Instituto Superior Técnico, Lisboa, Portugal, 2018.

[11] D.K. Cheng, "Field and Wave Electromagnetics", in Tsinghua University Press e Pearson Education Asia Ltd. (2nd ed.), 2006.

[12] J.A. Weldon, *A Direction Finding System Using Log Periodic Dipole Antennas in a Sparsely Sampled Linear Array*, Master's Thesis, Wright State University, Dayton, USA, 2010.

[13] D. Poljak, V. Doric, M. Birkie e D. Kosor, "Analysis of Log-Periodic Dipole Arrays with Boundary Elements", WIT Transactions on Modelling and Simulation, Vol 47, 2008, p. 75-84.

[14] J. Rajendran e G.A.S. Sundaram, "Design and Evaluation of Printed Log Periodic Dipole Antenna for L band Electrically Steerable Array System", in *1st International Conference on Computational Systems and Communications*, Trivandrum, India, Dec 2014.

[15] D.E Kerr, "Propagation of Short Radio Waves", in Peter Peregrinus Ltd, London, England, 1987.

[16] C. Haslett, "Essentials of Radio Wave Propagation", in Cambridge University Press, New York, USA, 2008.

[17] C.A. Fernandes, "Aspectos de Propagação na Atmosfera", Support text for the Radiopropagação discipline, Instituto Superior Técnico, Lisboa, Portugal, 2002.

[18] S.D.D. Pereira, *Propagação e Radiação de Ondas Eletromagnéticas em Ambientes Urbanos*, Master's Thesis, Instituto Superior Técnico, Lisboa, Portugal, 2014.

[19] C.A. Fernandes, Radiopropagação – Theoretical classes, Instituto Superior Técnico, Lisboa, Portugal, 2017.

[20] L.W. Nyback, "NORMAC 7000 ILS – ILS Principles and Equipment Theory", in Park Air Systems AS. Peterborough, United Kingdom, 2002.

[21] Visão Magazine, "Governo avança para novo aeroporto no Montijo", Feb. 2017 (http://visao.sapo.pt/actualidade/portugal/2017-02-15-Governo-avanca-para-novo-aeroporto-no-Montijo).

[22] N.F. Santos, "Tamanho da pista da base do Montijo é insuficiente para descolagem de aviões grandes", Público Newspaper, Mar. 2017 (https://www.publico.pt/2017/03/16/local/noticia/tamanho-da-pista-da-base-do-montijo-e-insuficiente-para-descolagem-de-avioes-grandes-1765474).

S. A. Rodrigues was born on February 4th, 1993, in Caldas da Rainha.

In 2011, she completed High-School at Escola Secundária de Peniche. In 2013, she joined the Portuguese Air Force Academy where she is currently finishing the Master's degree in Military Aeronautics, specialty of Electrical and Computer Engineering, area of Telecommunications.